Pflügers Arch – Eur J Physiol (1995) 430 : 745–750

ORIGINAL ARTICLE

Fabio Mammano · Corné J. Kros · Jonathan F. Ashmore

Patch clamped responses from outer hair cells in the intact adult organ of Corti

Received: 23 January 1995/Received after revision and accepted: 8 March 1995

Abstract Outer hair cells (OHCs) from the mammalian cochlea act as both sensory cells and motor cells. We report here whole-cell tight seal recordings of OHC activity in their natural embedding tissue, the intact organ of Corti, using a temporal bone preparation. The mean cell resting potential, -76 ± 4 mV ($n = 19$) and input conductance (10 ± 3 nS at -70 mV) of third turn hair cells were significantly lower than have been found in isolated cells. Two main K^+ currents in the cell were identified. One current, activated positive to -100 mV, was reduced by 5 mM $BaCl_2$. The other current, activated above -40 mV, was reduced by 100 μM 4-aminopyridine (4-AP) and by 30 mM tetraethylammonium (TEA). Both of these currents have been also identified in recordings reported from isolated cells. On stepping to different membrane potentials, cells imaged in the organ of Corti changed length by an amount large enough to cause visible distortions in neighbouring cells. By quantifying such distortions we estimate that the forces generated by OHCs can account for the enhanced response to sound required by the cochlear amplifier.

Key words Hair cells · Patch clamp · Cochlea · Mechanotransduction · Potassium currents · Digital imaging · Basilar membrane · Hearing

F. Mammano[1] · J. F. Ashmore (✉)
Department of Physiology, School of Medical Sciences, University Walk, Bristol BS8 1TD, UK

C. J. Kros
School of Biological Sciences, University of Sussex, Brighton BN1 9QG, UK

Present address:
[1]Biophysics Laboratory, S.I.S.S.A., Via Beirut 2–4, I-34014 Trieste, Italy

Introduction

It has been known for over a decade that auditory tuning in mammals relies upon a physiologically vulnerable mechanism [14, 21, 22, 27] named the "cochlear amplifier" [9]. According to the amplifier hypothesis, outer hair cell (OHC) receptor potentials elicited by sound-induced transducer currents (forward transduction) result in a mechanical feedback being applied to the cochlear partition by the induced changes in cell length (reverse transduction) and thus enhance vibration of the basilar membrane [2, 6, 8, 23]. Underlying such motile responses of OHCs is a specialized motor, revealed by a charge movement across the plasma membrane occurring when the membrane potential is stepped. The charge movement can be measured as a a non-linear contribution to the cell capacitance [3, 4, 25].

The potential changes in OHCs in the intact cochlea are determined by the ionic properties of the basolateral membrane. However, most of the present information about the ionic currents in OHCs is derived from patch clamp studies of isolated cells [2, 5, 13, 26] and there have been doubts about whether the reported currents and motility also occur in the intact cochlea. In this paper we resolve the issue directly by recording from undissociated OHCs in the their natural embedding tissue, the adult organ of Corti of an intact cochlear partition [28]. We show that, although the currents found in isolated cells are also present here, there are some significant differences. In particular, cells exhibit more negative resting potentials and a reduced leak current. A further advantage of the preparation is that it becomes possible to measure the distortions produced in the organ of Corti by the voltage-induced length changes in OHCs. This allows us to provide further support for the cochlear amplifier hypothesis.

Materials and methods

Tissue preparation

Adult albino guinea-pigs (350–600 g) were killed by rapid cervical dislocation. After dissecting the temporal bone, the bulla was opened and firmly held by attaching the bone with dental acrylic to a perspex chamber perfused with oxygenated phosphate buffer (PBS). To obtain access to cochlear turn 3, the partition in turn 4 was observed from scala media under low magnification by gently scraping away the bony wall of the cochlea. Access to turn 3 was then obtained by removing the overlying turn. Reissner's membrane was carefully peeled off leaving the partition intact. Cells in the partition were illuminated by a 1 mm fibre optic gently pushed to the outside of the cochlear wall and viewed using a 40 × 0.75 NA W.I. objective (Zeiss). With suitable positioning, this allowed a clear view of apical and basolateral membranes of the cells. Experiments were conducted at a temperature of 24–28°C.

Solutions

All solution changes could be made within 1 min. The external solution (PBS) contained (in mM): NaCl, 142; KCl, 4.0; $CaCl_2$, 1.0; $MgCl_2$, 2.0; Na_2HPO_4, 8.0; NaH_2PO_4, 2.0; adjusted to pH 7.3 with NaOH and osmolality 325 ± 2 mosmol/l with D-glucose. Control experiments to assess the effects of Mg^{2+} were performed in PBS containing up to 10 mM $MgCl_2$ and 1 mM $CaCl_2$. There were no appreciable differences in the recorded currents. When testing the effect of 5 mM Ba^{2+}, cells were initially bathed in PBS containing 1 mM $CaCl_2$ and 4 mM $MgCl_2$ and then washed through for 2–3 min with an otherwise identical iso-osmotic solution in which 5 mM 4-(2-hydroxyethyl)-1-piperazineethanesulphonic acid (HEPES) substituted for the phosphates. HEPES solution with 5 mM $BaCl_2$ and no other divalent cations was then applied for up to 15 min, followed by return to PBS. Nominal zero-Ca^{2+} buffers were comprised of PBS with 3 mM $MgCl_2$ and no added $CaCl_2$. Tetraethylammonium chloride (TEACl, 30 mM) replaced an equal concentration of NaCl in PBS. Drugs applied in the micromolar concentration range [4-aminopyridine (4-AP), dihydrostreptomycin] were simply added to normal PBS. All drugs were obtained from Sigma.

Data acquisition

Pipettes were pulled on a two-stage vertical puller (Narishige PP-83) from 1.5-mm o.d. soda glass (Clark, UK). They were filled with a solution containing (in mM): KCl, 144; $MgCl_2$, 2.0; ethylenebis(oxonitrilo)tetraacetate (EGTA) 5.0; Na_2HPO_4, 8.0; NaH_2PO_4, 2.0, adjusted to pH 7.2 with KOH and brought to 325 mosmol/l with D-glucose. The pipette resistance was typically 3 MΩ when measured in the bath. Conventional whole-cell recording techniques were employed, using an EPC/7 patch clamp amplifier (List Medical, Darmstadt, Germany). Current and voltage were sampled at either 2.5 kHz or 25 kHz using a standard laboratory interface (CED 1401plus, Cambridge Electronic Design, UK) under control of software written in house. Potentials were corrected for measured liquid junction potentials (typically −4 mV).

Images of the cells in situ were acquired by digitizing the output of a CCD camera (Wat-902, Watek, Japan) and storing the resulting image using a video store device (Arlunya TF6000, Dindima, Australia); acquisition could be triggered during the command steps.

Results are expressed as mean ± SD.

Results

Whole-cell OHC currents

Under direct visual control, patch pipettes were carefully advanced through the thin layer of Hensen's cells near the tectorial membrane border. Whole-cell tight seal recordings were made from the third row of OHCs adjacent to the Hensen's cells. Unless otherwise stated, data were derived from recordings of 19 cells in 12 preparations. All cells reported were located in the third cochlear turn at a site which, in the guinea-pig, is tuned to approximately 2 kHz [16].

On patch rupture the pipette recorded a zero-current potential of −30 mV to −40 mV, which rapidly became more negative as the pipette contents equilibrated with the cell interior over 30–60 s. After stabilization, the mean zero-current potential recorded under whole-cell conditions was −76 ± 4 mV (n = 19; range −69 mV to −85 mV). This is comparable to the value of −70 mV found in vivo using microelectrodes [7]. Cells were held close to this stable zero-current potential. The cell capacitance, measured by electronically cancelling the charging transient evoked by a −10-mV step from the resting potential, was 31 ± 3 pF,

Fig. 1A–C Whole-cell patch clamp recording from outer hair cells (OHCs) inside the intact organ of Corti at the third turn, third row, near the 2 kHz site. **A** *Top*: applied voltage commands, corrected for series resistance (9 MΩ). *Bottom*: current responses. Sampling = 2.5 kHz. The *dotted line* in this and subsequent figures shows position of zero current. **B** Current/voltage (I/V) relationship obtained from current and voltage values in (**A**) 5 ms before command offset. The *arrows* at −100 mV and −40 mV indicate the inflections where two current components become activated. See text for details. **C** Rapid current transient in OHCs produced at the onset of depolarizing steps (shown above). Sampling rate = 25 kHz. *Numbers* by each trace indicate the effective clamp step from a holding potential of −56 mV

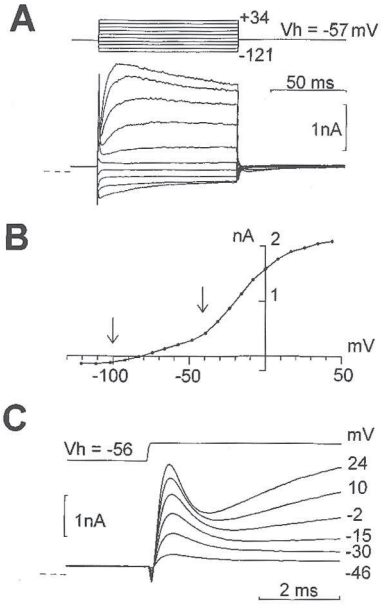

appropriate for cells about 50 μm long [13]. The average (uncompensated) pipette access resistance was 10 ± 3 MΩ (range: 7–18 MΩ).

Figure 1 shows typical voltage and current records obtained from cells from cochlear turn 3. For depolarizing commands, the recordings were characterized by a slowly developing outward current which reached a maximum in 10–20 ms.

Hyperpolarizing steps elicited an inward current which decayed more slowly, but with a variable time constant (10–30 ms) depending on membrane potential (Fig. 1A). The steady-state current/voltage relationship (I/V) was measured at the end of each 100-ms step command from a holding potential near rest (Fig. 1B). The slope conductance of the I/V curve at −70 mV was 10 ± 3 nS (range: 4–15 nS). The maximum slope conductance, 49 ± 22 nS (range: 22–106 nS), was reached at a potential of −21 ± 6 mV (range: −6– −29 mV). The records show a small leak current present at potentials negative to −100 mV. The leak corresponded to a conductance of 2.9 ± 1.6 nS measured at −110 mV. This leak has not been subtracted from the records below because of its small size. It is significantly smaller than in isolated cells where the leak can be much larger [13]. As will be seen below, a fraction of this leak is likely to have been due to the non-selective transducer channels in the apical membrane.

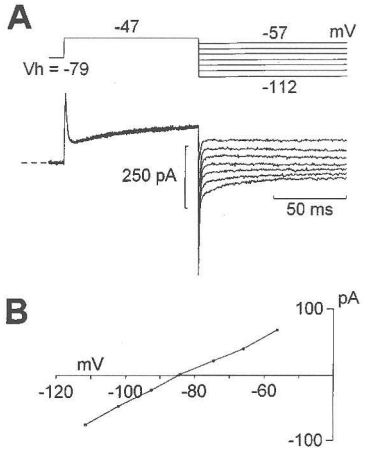

Fig. 2A,B Reversal potential measurement. **A** *Top*: applied voltage commands, corrected for series resistance (9 MΩ). *Bottom*: tail currents elicited by pre-stepping the potential to −24 mV from rest (−72 mV). **B** *Abscissa*: post-step potentials. *Ordinate*: leak-subtracted currents measured 10 ms after pre-step offset, showing reversal at −79 mV. Leak conductance was estimated by measuring the difference between the tail currents obtained at the two most negative potentials (data in **A** and **B** are from the same cell). Similar results were obtained for all cells studied in this way

Fast transient currents in OHCs in situ

In addition to the outward currents, a fast transient current was present at the onset and offset of the command step. In isolated OHCs this current is closely related to the motor function of the cells [3, 4, 25] Figure 1C shows that the amplitude of the transient was dependent upon the size of the voltage step, as observed in isolated cells. The kinetics were also voltage dependent [25]. For a typical access resistance of 10 MΩ, the transients peaked within between 0.7 ms and 0.5 ms and relaxed within between 0.8 ms and 0.4 ms over the range of −50 mV to +30 mV. Integration of the current yielded a maximum charge transfer of 1.8 pC at command onset, a value comparable to that described in isolated cells.

K^+ currents in OHCs in situ

As was apparent from the I/V curve, at least two currents were activated over different voltage ranges (Fig. 1B). The first component activated positive to −100 mV and was shown as an inflection of the I/V curve at −100 mV. The second component activated above −40 mV and was responsible for the increase in the slope of the I/V curve. Although there are significant differences between cells from different cochlear turns (F. Mammano and J. F. Ashmore, in preparation), this two-stage activation pattern was a common feature of all the cells studied in cochlear turn 3.

Analysis of the tail currents indicates that both of these two currents were carried by K^+. Figure 2 shows that the tail currents obtained upon stepping to a negative potential after a constant depolarizing step to between −50 mV and −20 mV reversed at −80 ± 3 mV (n = 13), close to the expected value for the reversal potential of K^+ (E_K = −92 mV).

The first current component identified in the I/V curve was activated at resting potentials (−76 mV) and was deactivated upon hyperpolarization (Figs. 1B, 3A). In having this voltage dependence it is similar to $I_{K,n}$, the main K^+ current, described previously in isolated OHCs [13], activated near rest. It was partially blocked by 5 mM external Ba^{2+} (Fig. 3A, bottom); the effect was reversible. Superfusion with zero Ca^{2+} alone did not signifiicantly affect this current. Consistent with the block, 5 mM Ba^{2+} shifted the zero-current potential of recorded cells by 10 mV or more in the depolarized direction (Fig. 3B). The currents activated by depolarization were also reduced, by about 60% at 0 mV, in 5 mM Ba^{2+} (n = 3).

The second current component, activated at potentials positive to −40 mV, was reversibly suppressed by 100 μM 4-AP when applied externally. In contrast, 4-AP produced no appreciable reduction of $I_{K,n}$ and left the zero-current potential unaffected (Fig. 3D). To characterize the outward currents further, the bath solution was washed out with one containing nominally zero external Ca^{2+}. The results suggest that a Ca^{2+} activated K^+ conductance activating above −35 mV as

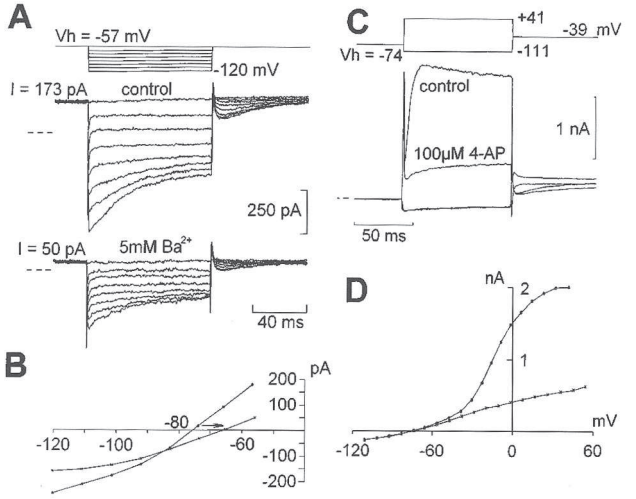

Fig. 3A–D Identification of the main cell conductances. **A** *Top*: applied voltage commands, corrected for series resistance (7 MΩ). *Middle*: control currents. *Bottom*: currents in 5 mM external Ba^{2+}. **B** Steady-state *I*/*V*s from traces in **A**. *Circles*: control; *crosses*: Ba^{2+}. Note the positive shift of the zero-current potential (*arrow*) due to reduction in the conductance activated at rest. **C** *Top*: applied voltage commands, corrected for series resistance (8 MΩ). *Bottom*: currents obtained with and without 100 µM external 4-aminopyridine (4-AP). Notice that the outward current activating above −40 mV was completely blocked (the maximum slope conductance decreased seven fold from 41 nS at −17 mV to 6 nS at −29 mV) whereas inward currents and zero-current potential were unaffected. **D** Comparison of steady-state *I*/*V* curves between −120 mV and +60 mV. Data from cell in **C**. *Circles*: control; *crosses*: 4-AP

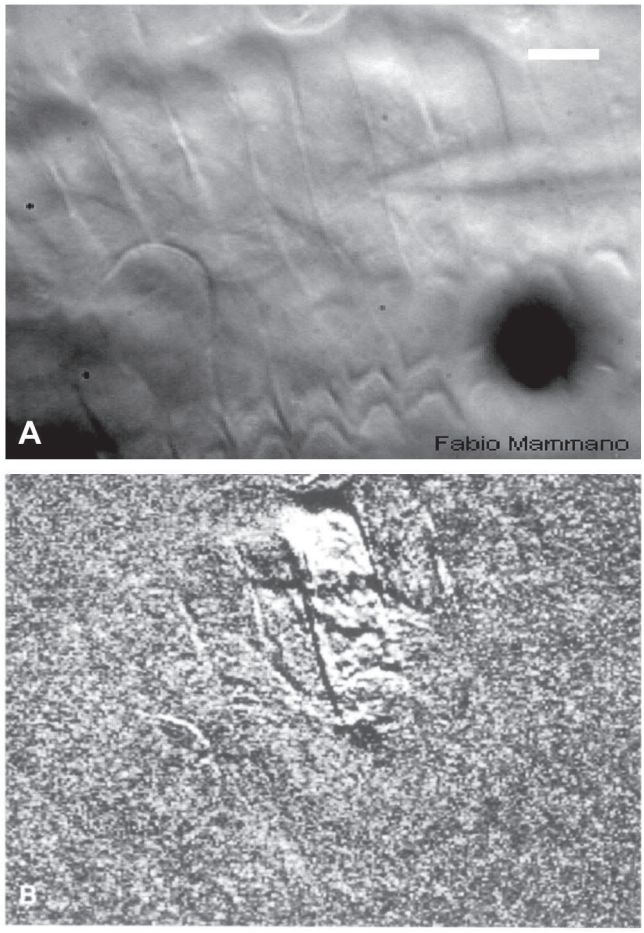

Fig. 4A,B OHCs shorten when depolarized within the organ of Corti. **A** Digital image of the cochlear partition viewed from scala media at an angle, bringing the full length of OHCs into focus. The image is 256 × 256 pixels (resolution 356 nm/pixel). It shows a patch pipette entering from the right and attached to a third row outer hair cell (unstimulated). Cell stereocilia are visible, through the intact tectorial membrane, at the bottom of the frame. *Scale bar*: 10 µm. **B** Difference image obtained by pixel-by-pixel subtraction of the image in **A** and a second image obtained 30 ms after stepping the potential to 0 mV (corrected for series resistance) from a holding potential of −80 mV. Total command duration = 100 ms. Only those parts of the cell which alter between frames stand out of pixel boxes along the cell axis

in isolated OHCs [13], made only a small contribution to the outward currents, measured under our experimental conditions. TEA (30 mM) reduced the outward currents by about 30% at 0 mV ($n = 4$) with negligible effects on the resting potentials and $I_{K,n}$. However, the kinetics of the residual outward current present in TEA differ from those obtained in 4-AP, suggesting that the current activating above −40 mV may be further subdivided by these agents.

Although these two K^+ currents describe the main properties of the *I*/*V* curve, further experiments suggested that the transducer channels themselves may make a small contribution to the *I*/*V* curve at potentials negative to −50 mV. External application of 100 µM dihydrostreptomycin, a known blocker of the transducer, hyperpolarized the cell by 6 mV and decreased the resting conductance by approximately 2 nS ($n = 3$). This suggests that a small fraction (less than 5%) of the total conductance was probably contributed by the transducer channels associated with the stereocilia.

Length changes of OHCs in situ

A significant attribute of OHCs is their motility. This property has been described most completely in isolated cells and an outstanding question is whether it occurs when the cell is left in the organ of Corti. Figure 4 shows that when the cells were simultaneously patched and visually recorded in situ, the currents elicited under voltage clamp conditions were accompanied by measurable changes in length. For typical depolarizing commands of between 50 mV to 100 mV from rest, the cell shortened by up to 1.5 µm. An appreciable displacement of neighbouring third row cells was also apparent. This was best seen by digital subtraction of the images (Fig. 4B). There was no evidence in the current records for direct electrical coupling between hair cells and thus distortions of the cochlear partition induced by stimulating a single cell were

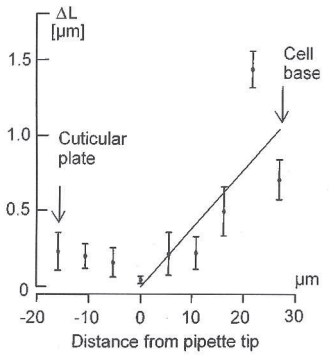

Fig. 5 Cell shortening versus distance from patch-pipette tip. Data measured by averaging the difference image intensity over 7.2 μm × 7.2 μm windows for +80 mV steps from rest for $n = 3$ cells. *Vertical bars* = SEM. The largest displacements were found towards the cell base, whereas virtually no motion was observed near the pipette tip. The displacement scale was calibrated by measuring the shift in the pixel profile of the base of the cell between images. The *continuous line* (slope 12.0 nm/mV) is a least-squares fit to the data from 0 μm to 30 μm, through the origin, defined as the position of the pipette tip.

mechanically propagated over a range of between 10 μm and 20 μm on each side of the cell.

The largest potential-induced displacements were found towards the cell base, whereas virtually no motion was observed near the pipette tip. Figure 5 shows that when the motion was measured, the sensitivity to potential steps applied was 12.0 ± 1.7 nm/mV. Both cell poles moved towards the patch pipette, consistent with the proposal [8, 12] that the hair cell motor is distributed along the length of the basolateral membrane.

Discussion

Differences between in situ and isolated OHCs

Compared to cells in isolation, OHCs in the intact organ of Corti exhibit more hyperpolarized zero-current potentials (−76 mV as opposed to −45 mV [26] and −57 mV [13]) and lower leak and input conductances. The maximum slope conductance (45 nS),even after leak subtraction, is also considerably larger than can be calculated from recordings of isolated cells of similar length (about 18 nS for a 50-μm-long cell [13]). The maximum slope conductance values for these third row OHCs are similar to those of cultured neonatal OHCs from the mouse [24].

The properties of $I_{K,n}$ in situ appear to be similar to those described elsewhere in isolated OHCs [13]. This current component is not an inward rectifier but is substantially activated at the resting potential of the cells. It contributes to the outward current in response to depolarizing voltage steps whilst hyperpolarization causes it to deactivate.

The outward K^+ current, which activates above −40 mV and which is blocked by 4-AP and TEA, resembles kinetically the currents described in isolated mature OHCs [13, 26] and immature OHCs from newborn mice [24]. Block of this current by 4-AP is consistent with recordings from dissociated cells [19] and argues against it being due exclusively to a Ca^{2+}-activated K^+ channel. Nevertheless, it remains to be established whether a component of this current is affected by extracellular Ca^{2+} under the conditions observed in isolated cells [13].

Implications for cochlear mechanics

As described in the Materials and methods, following the removal of Reissner's membrane, the intact cochlear partition was bathed in artificial perilymph. Although this resulted in perilymph bathing the apical surface of the hair cells, electromotile responses are known to be insensitive to alteration of the bathing medium facing the stereocilia [10, 16, 17]. Therefore, the present observations can be used to make inferences about how the cochlea responds to sound.

The favoured mechanism for amplification within the cochlea is one where reverse transduction opposes the dissipative, viscous damping of the basilar membrane motion [11, 15, 20]. This requires the three OHCs in adjacent rows within each transverse section of the organ of Corti to produce forces at least comparable in magnitude and opposed in phase to the viscous forces developed mainly in the narrow subtectorial space by the shearing between the tectorial membrane and reticular lamina [18].

The present data revise the magnitude of the forces that OHCs are capable of producing under normal sound-stimulated conditions. Since the static stiffness K_c of a 50-μm-long OHC is estimated to be approximately 540 pN/μm [12], the three rows of OHCs at the 2 kHz site will have a combined stiffness of 3 × 0.540 = 1.6 nN/μm. Measurements made using transcochlear current suggest that the stiffness of the remaining components of the partition is comparable to that of the hair cells [16] and, thus, in each section, the static stiffness of the cochlear partition would be about 3.2 nN/μm. The measured sensitivity of the OHC motor for this region of the cochlea is 12 nm/mV (Fig. 5). Therefore, the present data indicate that, in each cochlear section, the motor can generate at least 3.2 nN/μm × 12 nm/mV = 38 pN/mV.

Our patch recordings show that at the mean resting potential found in vivo (−70 mV [7]) the cell input resistance is 100 ± 33 MΩ, i.e. a factor of 5 greater than that measured with conventional microelectrodes. The AC receptor potential, measured in turn 3 in vivo near the 1 kHz site is 3 mV at 40 dB SPL [7]. Up to this sound level the cochlear amplifier acts linearly. Therefore, we may increase this value by 5 times and find that the force generated by the OHCs would be 580 pN per section. At 2 kHz and 40 dB SPL the

viscous forces opposing motion that are generated within the cochlear partition can be estimated at about 300 pN per section. This is because, ignoring edge effects, the viscous force between two plates of area A and separation d in a fluid of viscosity η is $F_v = \eta A\, 2\pi f\, D/d$ when undergoing shear displacement of amplitude D at a frequency f [1]. Applying this formula to a single section of the cochlear partition where the height of the subtectorial gap is $d = 1$ μm, $A = 100$ μm × 10 μm and using a viscosity $\eta = 1.5$ cP, we find $F_v = 340$ pN at a frequency $f = 2$ kHz and at a displacement $D = 20$ nm, referred to the basilar membrane (equivalent to 40 dB SPL).

Because of the inertial reaction of the tectorial membrane, the OHC membrane potential at the appropriate characteristic frequency is expected to be 90° out of phase with the displacement (see [18], Eq. 18). Thus the present data show that OHCs, at least in the apical turns, are more than capable of generating sufficient force to alter cochlear mechanics by cancelling the viscous damping of the partition.

Acknowledgements Supported by the Wellcome Trust and the EC (Basic Research Action, SSS 6961). C.J.K. is a Royal Society University Research Fellow. We thank Drs. Paul Kolston and Jonathan Gale for their critical comments on the manuscript.

References

1. Allen JB (1980) Cochlear micromechanics - a physical model of transduction. J Acoust Soc Am 68:1660–1670
2. Ashmore JF (1987) A fast motile response in guinea-pig outer hair cells: the cellular basis of the cochlear amplifier. J Physiol (Lond) 388:323–347
3. Ashmore JF (1989) Transducer motor coupling in outer hair cells. In: Wilson JP, Kemp DT (eds) Cochlear mechanism: structure, function and models, Plenum, New York, pp 107–113
4. Ashmore JF (1992) Mammalian hearing and the cellular mechanism of the cochlear amplifier. In: Corey DP, Roper SD (eds) Sensory transduction. The Rockefeller University Press, New York, pp 396–412
5. Ashmore JF, Meech RW (1986) Ionic basis of membrane potential in outer hair cells of the guinea-pig cochlea. Nature 322: 368–371
6. Brownell WE, Bader CR, Bertrand D, de Ripaubierre Y (1985) Evoked mechanical responses of isolated cochlear hair cells. Science 227:194–196
7. Dallos P (1985) Response characteristics of mammalian cochlear hair cells. J Neurosci 5:1591–1608
8. Dallos P, Evans BN, Hallworth R (1991) Nature of the motor element in electrokinetic shape changes of cochlear outer hair cells. Nature 350:155–157
9. Davis H (1983) An active process in cochlear mechanics. Hear Res 9:79–90
10. Evans BN, Hallworth R, Dallos P (1988) Outer hair cell motility in an appropriate ionic environment. Soc Neurosci Abstr 14:800
11. Geisler CD (1991) A cochlear model using feedback from motile outer hair cells. Hear Res 54:105–117
12. Holley MC, Ashmore JF (1988) A cytoskeletal spring in outer hair cells. Nature 355:635–637
13. Housley GD, Ashmore JF (1992) Ionic currents of outer hair cells isolated from the guinea-pig cochlea. J Physiol (Lond) 448:73–98
14. Khanna SM, Leonard D (1982) Basilar membrane tuning in the cat cochlea. Science 215:305–306
15. Kim DO (1986) Active and nonlinear cochlear biomechanics and the role of outer-hair-cell subsystem in the mammalian auditory system. Hear Res 22:105–114
16. Mammano F, Ashmore JF (1993) Reverse transduction measured in the isolated cochlea by laser Michelson interferometry. Nature 365:838–841
17. Mammano F, Ashmore JF (1995) A laser interferometer for sub nanometre measurements in the cochlea. J Neurosci Methods (in Press)
18. Mammano F, Nobili R. (1993) Biophysics of the cochlea: linear approximation. J Acoust Soc Am 93:3320–3332
19. Nakagawa T, Kakehata S, Akaike N, Komune S, Takasaka T, Uemura T (1992) Voltage-dependent channels in dissociated outer hair cells of guinea pig. Proc Sendai Symp 2:31–35
20. Neely SR, Kim DO (1986) A model for active elements in cochlear biomechanics. J Acoust Soc Am 79:1472–1480
21. Nuttall AL, Dolan DF, Avinash G (1990) Measurements of the basilar membrane tuning with laser Doppler velocimetry. In: Dallos P, Geisler CD, Matthews JW, Ruggero MA, Steele CR (eds). The mechanics and biophysics of hearing. Springer, Berlin Heidelberg New York pp 288–295
22. Ruggero M, Rich N (1991) Furosemide alters organ of Corti mechanics: evidence for feedback of outer hair cells upon the basilar membrane. J Neurosci 11:1057–1067
23. Ruggero M (1992) Response to sound of the basilar membrane of the mammalian cochlea. Curr Opin in Neurobio 2:449–456
24. Rüsch A, Kros CJ, Richardson GP, Russell IJ (1991) Potassium and calcium currents in outer hair cells in organotypic cultures of the neonatal mouse cochlea. J Physiol (Lond) 434:52P
25. Santos-Sacchi J (1991) Reversible inhibition of voltage-dependent outer hair cells motility and capacitance. J Neurosci 11:3096–3110
26. Santos-Sacchi J, Dilger JP (1988) Whole-cell currents and mechanical responses of isolated outer hair cells. Hear Res 35:143–150
27. Sellick PM, Patuzzi RB, Johnstone BM (1982) Measurement of basilar membrane motion in the guinea pig using the Mössbauer technique. J Acoust Soc Am 72:131–141
28. Ulfendahl M, Khanna SM, Flock Å (1989) A temporal bone preparation for the study of cochlear micromechanics at the cellular level. Hear Res 40:55–64